Russian Journal of General Chemistry, Vol. 74, No. 6, 2004, pp. 842–859. Translated from Zhurnal Obshchei Khimii, Vol. 74, No. 6, 2004, pp. 915–932.

Synthesis and Comparative Analysis of the Steric and Supramolecular Structures of Diastereomers of 4,4-Bis(trifluoromethyl)-2-(fluoroalkoxy)-6,7-benzo-1,3,2λ^5-dioxaphosphepin-5-one 2-Oxides

A. T. Gubaidullin, V. F. Mironov, L. M. Burnaeva, I. A. Litvinov, A. B. Dobrynin, E. I. Goryunov, G. A. Ivkova, I. V. Konovalova, and T. A. Mastryukova

Arbuzov Institute of Organic and Physical Chemistry, Kazan Research Center, Russian Academy of Sciences, Kazan, Tatarstan, Russia

Kazan State University, Kazan, Tatarstan, Russia

Nesmeyanov Institute of Organoelement Compounds, Russian Academy of Sciences, Moscow, Russia

Received May 29, 2002

Abstract — Reaction with hexafluoroacetone of 2-fluoroalkoxy-5,6-benzo-1,3,2-dioxophosphorinan-5-ones containing a chiral fluorinated exocyclic substituent on the phosphorus atom, with hexafluoroacetone leads to formation of 4,4-bis(trifluoromethyl)-6,7-benzo-1,4,2-dioxaphosphepines with a high regio- and stereoselectivity. The configuration of all isolated individual diastereomers was established by X-ray diffraction. The molecular and supramolecular structure of the compounds were examined in terms of the proposed model that takes account of the revealed effect of separation of hydrophilic and lipophilic regions in the crystal.

Phosphorylated derivatives of salicylic acid (5,6-benzo-1,3,2-dioxaphosphorinan-4-ones or "salicyl phosphites") contain a highly reactive P–O–C(O) fragment are promising reagents for preparing seven-membered functionalyzed P-heterocycles, such as 6,7-benzo-1,3,2-dioxa-, 6,7-benzo-1,4,2-dioxa-, 6,7-benzo-1,3,2-oxaza-, and 6,7-benzo-1,4,2-oxazaphosphepines, as well as 6,7-benzo-1,2-oxaphosphepines [1–10] hardly available by other methods. This synthesis is based on the regio- and stereoselective reactions involving expansion of the starting phosphorinane ring to phosphepine under the action of compounds containing C=O, C=C, or C=N bonds, such as esters of mesoxalic, trifluoropyruvic, pyruvic, benzoylformic, arylcarbonylphosphonic, and benzylidenemalonic acids, chloral, trifluoroacetone, hexafluoroacetone imine, and aldimines.

This contribution presents the results of investigation of the reaction with hexafluoroacetone of structurally more complex diastereomeric salicyl phosphites **I**–**VI** containing fluorinated alkoxyl radicals with a chiral carbon atom as the exocyclic substituent on phosphorus (for preliminary reports, see [11]).

The use of diastereomeric derivatives **I**–**VI** permits to solve some problems concerning the stereochemistry of phosphepine formation, since the reaction with hexafluoroacetone involves directly the chiral phosphorus atom. Starting salicyl phosphites **I**–**VI** were obtained as diastereoimeric mixtures ($d_1 : d_2$ ~ 1 : 1) by phosphorylation of related racemic fluorinated carbinols with 2-chloro-5,6-benzo-1,3,2-dioxaphosphorinan-4-one. Their structure was confirmed by spectral methods (see Experimental).

Compounds **I**–**VI**, like "ordinary" salicyl phosphites studied previously [12], easily react with hexafluoroacetone to give diastereomeric 4,4-bis-(trifluoromethyl)-6,7-benzo-1,3,2-dioxaphosphepines **VII**–**XII** in practically quantitative yields. The distereomeric ratio is the same as in the starting phosphites. This fact tells in favor of a highly stereoselective formation of the phosphate center from the P(III) atom.

1,3,2-Dioxaphosphepines **VII**–**XII** are viscous colorless oils. Their $^{31}P–\{^1H\}$ NMR spectra contain two upfield signals at δ_P –15 to –17 ppm, characteristic of 4,4-bis(trifluoromethyl)-6,7-benzo-1,3,2-dioxaphosphepines [12]. The IR spectrum of the diastereomers contains one or several intense bands at 1700–1730 cm^{-1}, characteristic of stretching vibrations of a keto group bound with a fluorinated substituent.

1070-3632/04/7406-0842

Table 1. ^{13}C–{^{1}H} NMR spectral parameters of phosphepines **VIII** and **XII**, δ, ppm (*J*, Hz)

Atom no.	Compound **VIII**,[a] δ, ppm (*J*, Hz) (acetone-d_6)	Compound **XII**,[a] δ, ppm (*J*, Hz) ($CDCl_3$)
C^4	81.16 sept (sept) (29.0–29.1, $FC^{12}C^4$; 0, P^2OC^4)	83.94 sept.d (30.4, $FC^{12}C^4$; 8.2, P^2OC^4), 83.95 sept.d (30.7, $FC^{12}C^4$; 8.2, P^2OC^4) (d_1, d_2)
C^5	192.34 d (br.d) (0.93–1.0, $POCC^5$; 4.7, $HC^{11}CC^5$)	186.02 br.s (d_2), 186.0 br.s (d_1)
C^6	128.48 d (m) (1.5–1.6, $P^2OC^7C^6$)	127.58 br.s (d_1, d_2)
C^7	148.61 d (m) (5.4, POC^7)	147.75 d (8.2, POC) (d_1), 147.49 d (7.4, POC) (d_2)
C^8	120.60 d (d.d.d.d) (165.8, HC^8; 7.9, $HC^{10}CC^8$; 2.5, $POCC^8$; 1.4–1.5, HC^9C^8; 1.2–1.3, $HC^{11}CCC^8$)	121.90 d (6.6, POCC) (d_2), 121.56 d (6.7, POCC) (d_1)
C^9	133.31 d (d.d.m) (165.6, HC^9; 8.4, $H^{11}CC^9$; 1.5, $POCCC^9$)	136.84 s (d_1), 136.74 s (d_2)
C^{10}	124.73 d (d.d.m) (167.6, HC^{10}; 5.6–6.0, HC^8CC^{10}; 1.7, $POCCCC^{10}$)	127.50 s (d_1), 127.47 s (d_2)
C^{11}	129.47 br.s (d.m) (162.7–163.0, HC^{11}; 6.0–7.0, HC^9CC^{11})	131.96 d (1.5, POCCC), 131.81 d (1.4, POCCC) (d_1, d_2)
C^{12}, C^{13}	122.04 q.m (q.m) (289.5, FC^{12}; 1.1–1.2, $FC^{13}CC^{12}$)	119.63 q.m (289.0, FC) (d_1, d_2)
C^{14}	75.84 q.d (d.q.d.t) (151.8, HC^{14}; 34.2, FCC^{14}; 4.0–4.4, POC^{14}; 4.0, $HC^{17}CC^{14}$)	73.92 br.d.m (32.3–32.7, FCC) (d_2), 73.69 br.d.m (32.3–32.7, FCC) (d_1)
C^{15}	123.53 q.d (q.d.d) (280.6–281.0, FC; 9.8–10.0, POCC; 6.0–6.1, $HC^{14}C^{15}$)	17.21 br.d.d (4.8–5.0, POCC; 4.8–5.0, FCCC) (d_1), 16.90 br.d.m (4.8–5.0, POCC; 4.8–5.0, FCCC) (d_2)
C^{16}	134.12 d.q (m) (2.2, $POCC^{16}$; 1.0–1.2, $FC^{15}CC^{16}$)	89.89 d.m (212.4, FC; 25.7–28.5, FCC) (d_1, d_2)

[a] Parenthesized are the shapes of signals in the ^{13}C NMR spectra; C^{17}, 128.38 q (d.m) (167.2, HC^{17}; 1.0–1.2, $FC^{15}CCC^{17}$); C^{18}, 134.61 s (d.d.d) (9.9–10.0, $HC^{20}CC^{18}$; 3.9, $HC^{19}C^{18}$; 3.0, $HC^{17}C^{17}C^{18}$); C^{19}, 130.62 s (d.d.d) (167.3, HC^{19}; 7.9, $HC^{21}CC^{19}$; 4.9, $HC^{17}CC^{19}$; 1.4–1.5, $HC^{20}C^{19}$); C^{20}, 130.78 s (d), (165.0. HC^{20}); C^{21}, 127.06 q (d.m) (162.7, HC^{21}; 0.9–1.0, $FC^{15}CCC^{21}$).

[b] The C^{17}–C^{19} signals appear as very complex triplets of multiplets at 110.6 and 107.8 ppm (275.0-285.0, FC) (d_1, d_2).

The structure of certain 1,3,2-dioxaphosphepines (**VIII**, **XII**) was also confirmed by the ^{13}C NMR spectra (Table 1). The spectra contain characteristic downfield (δ_C 191–193 ppm) and upfield (δ_C 80–82 ppm) signals with expected multiplicities, providing unambiguous evidence for the presence of a P–O–$C(CF_3)_2$–C(O) fragment in the molecules of phosphepines **VIII**–**XII**. The spectra were assigned on the basis of ^{13}C and ^{13}C–{^{1}H} NMR experiments, as well as our previous results for structurally related 4,4-bis(trifluoromethyl)-6,7-benzo-1,3,2-dioxaphosphepines [12].

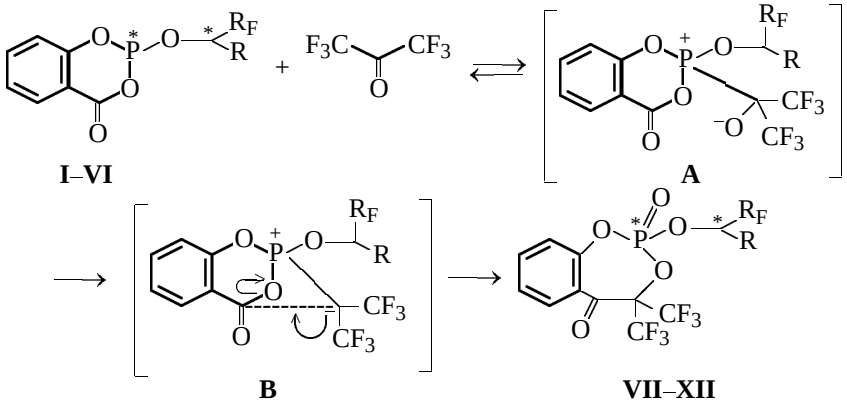

R_F = CF_3, R = Ph (**I, VII**), 3-Cl–C_6H_4 (**II, VIII**), 3-MeO–C_6H_4 (**III, IX**), 3-CF_3–C_6H_4 (**IV, X**); R_F = $CF_2CF_2CF_3$, R = Ph (**V, XI**); R_F = *cyclo*-C_6F_{11}, R = Me (**VI, XII**).

The reaction evidently involves initial nucleophilic attack of phosphorus on the carbonyl fragment of the highly electrophilic hexafluoroacetone. The resulting intermediate dipolar ion **A** containing a P–C bond undergoes $P^+–C–O^- \rightarrow P^+–O–C^-$ rearrangement to give dipolar ion **B** which stabilizes via intramolecular nucleophilic substitution at the carbon atom of the endocyclic carbonyl group.

All the prepared isomeric phosphepines **VII**–**XII** partially crystallized when kept in a mixture of ether and methylene chloride. The isolated crystals were individual diastereomers. Their purity was controlled by ^{31}P and ^{13}C NMR (compound **VIII**, Table 1) spectroscopy. Crystallization from acetone almost always provided single crystals suitable for X-ray diffraction analysis (compounds **VIII**–**XII**).

By now we have accumulated an abundant experimental evidence for the steric structure of unsymmetrical functional derivatives of seven-membered heterocycles, such as 6,7-benzo-1,3,2- and 6,7-benzo-1,4,2-dioxa(oxaza)phosphepin-5-ones [4–11, 13] containing both neutral and charged (anionic) phosphorus. Therefore, in this work we considered it expedient not only to discuss details of the steric structure of compounds **VIII**–**XII**, but also to compare them with our previous data for structures **XIII**–**XXVII**.

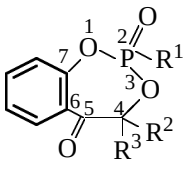

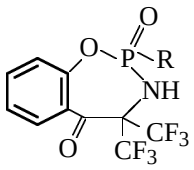

XIII–**XVII** **XVIII, XIX**

$R^1 = NEt_2$, R^2 = Ph, R^3 = COOEt (**XIII**); $R^1 = O^-Et_3NH^+$, $R^2 = R^3 = CF_3$ (**XIV**); R^1 = OEt, $R^2 = CF_3$, R^3 = COOMe (**XV**); R^1 = OH, R^2 = Ph, $R^3 = P(O)(OEt)_2$ (**XVI**); R = OH, R^2 = 4-ClC_6H_4, $R^3 = P(O)(OMe)_2$ (**XVII**); **R = NEt_2** (**XVIII**), Ph (**XIX**).

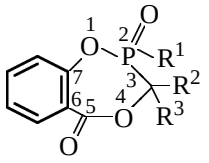

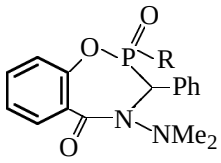

XX–**XXII** **XXIII**

$R^1 = OCH_2CF_2CHF_2$, $R^2 = CF_3$, R^3 = Me (**XX**); R^1 = Ph, R^2 = H, $R^3 = CCl_3$ (**XXI**); R^1 = OMe, R^2 = H, $R^3 = CCl_2$ (**XXII**); R = OC_6F_5 (**XXIII**).

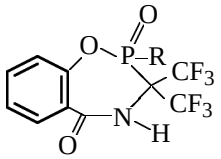

XXIV–**XXVI**

R = OMe (**XXIV**), $OCH_2CF_2CHF_2$ (**XXV**), $^-OEt_2NH_2^+$ (**XXVI**).

First of all note that no one of our studied molecules had a *chair* conformation of the seven-membered heterocycle, even though gas-phase calculations [6, 14] show that this conformation is close in stability to the unsymmetrical distorted *bath* or *twist-bath* conformations realized in most of the above molecules (in crystal). A specific feature of the molecules in hand is a planar $C^5C^6C^7O^1$ four-atomic fragment. The remaining P^4, C^3, and X^4 (X=O, N) atoms locate on the one side of this plane, deviating from it by different distances (in the *bath* conformation). The presence of this planar fragment in many aspects predetermines the *bath* conformation of 1,4,2-dioxa- and 1,4,2-oxazaphosphepines **XX**–**XXVI**. A specific feature of 1,3,2-dioxa- and 1,3,2-oxazaphosphepines **XIII**–**XIX** is that their heterorings can exist in three different conformations: distorted unsymmetrical *bath*, unsymmetrical *twist-bath* (with a $C^4C^5C^6C^7O^1$ five-atomic fragment and P^2 and X^3 deviating by different distances to one side from it), and unsymmetrical *twist* (with a planar $C^5C^6C^7O^1$ four-atomic fragment and P^2 and X^3 deviating to one side from it and C^4, to the opposite side; the deviation of X^3 from the base plane is insignificant). Evidently, 6,7-benzo-1,3,2λ^5-dioxaphosphepin-5-one 2-oxides and 6,7-benzo-1,3,2λ^5-oxazaphosphepin-5-one 2-oxides are much more conformationally labile than 6,7-benzo-1,4,2λ^5-dioxaphosphepin-5-one 2-oxides and 6,7-benzo-1,4,2λ^5-oxazaphosphepin-5-one 2-oxides.

The conformational behavior of substituents on phosphorus in these unsymmetrical heterocycles is largely determined by the general anomeric effect [15], but there are some exceptions. Hence, the diethylamino or ethoxy groups on phosphorus in crystalline 1,3,2-dioxaphosphepines **XIII** and **XV** have opposite orientations (pseudoaxial diethylamino group in **XIII** and pseudoequatorial ethoxy group in **XV**), what disagrees with the concept of the anomeric effect [15]. At the same time, the example of these two structures allows no prognostic conclusions as to the preferred orientation of substituents on the phosphorus atom. In this connection the investigation of five new 6,7-benzo-1,3,2-dioxaphosphepine derivatives **VIII**–**XII** that essentially complement the range of previously studied structures would provide further information for solving this problem.

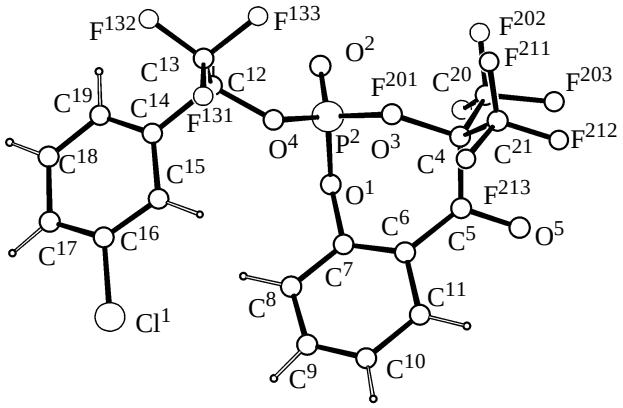

Fig. 1. Molecular geometry of phosphepine **VIII** in crystal and numbering scheme.

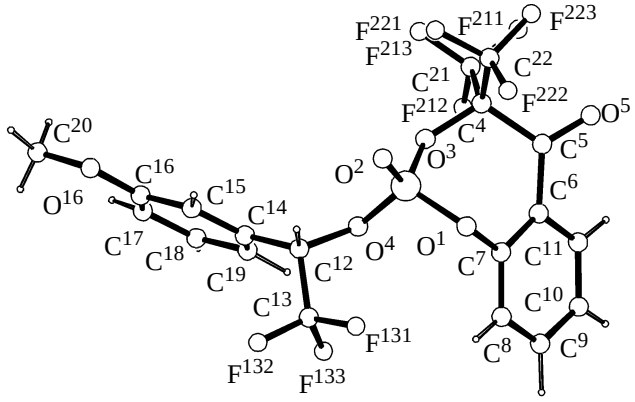

Fig. 2. Molecular geometry of phosphepine **IX** in crystal and numbering scheme.

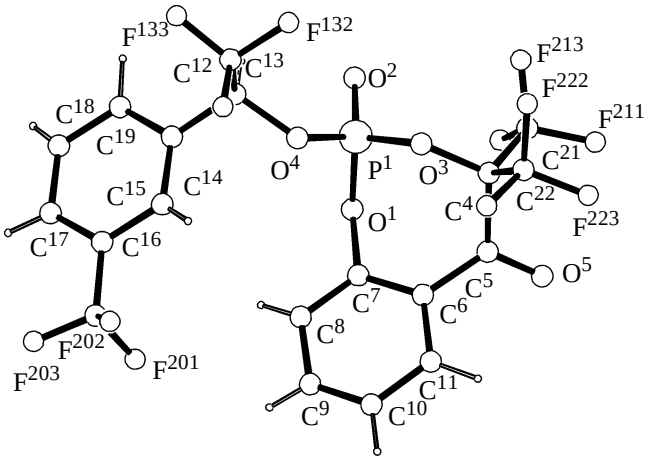

Fig. 3. Molecular geometry of phosphepine **X** in crystal and numbering scheme.

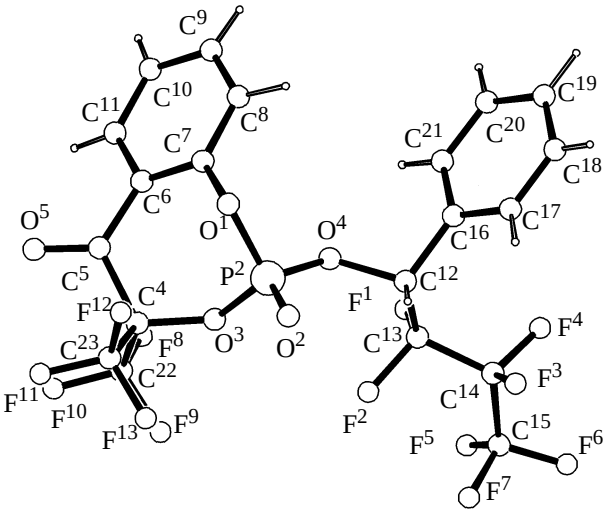

Fig. 4. Molecular geometry of phosphepine **XI** in crystal and numbering scheme.

The heteroring conformation in **VIII**–**XII** (Figs. 1–5) relate to the first type of conformations, i.e. a distorted unsymmetrical *bath* with a planar $C^5C^6C^7O^1$ fragment and P^2, O^3, and C^4 locating on one side of this plane at different distances from it (Table 2). The phosphoryl group in these compounds is pseudoequatorial and the substituted alkoxy groups are pseudoaxial. Like in our previous works [4–11, 13], to describe location of substituents on the phosphorus atom in such heterorings we use the terms

Table 2. Distances of selected atoms (Å) from the planar fragment $O^1C^7C^6C^5$ in molecules **VIII**–**XII** (parenthesized are rms deviations).

Atom	**VIII**	**IX**	**X**	**XI**	**XII**
P^2	1.240(7)	–1.2878(9)	1.2662(9)	–1.2295(6)	–1.2693(9)
O^3	1.72(1)	–1.741(2)	1.797(5)	–1.746(2)	–1.661(2)
C^4	0.85(2)	–0.973(3)	1.058(3)	–0.989(2)	–0.834(4)
O^5	–0.83(2)	0.616(3)	–0.799(3)	0.642(2)	0.598(5)
C^{20} (C^{22})	0.19(2)	–5.799(3)	2.144(4)	–8.369(3)	–1.859(4)
C^{21}	2.03(3)	–7.009(4)	0.406(4)	–2.077(3)	0.102(4)

Table 3. Selected torsion angles τ (deg) in molecules **VIII**–**XII** and puckering amplitudes of their seven-membered heterorings (*Q*, Å)

Angle	**VIII**	**IX**	**X**	**XI**	**XII**
$O^4P^2O^1C^7$	55(2)	57.5(2)	56.3(3)	53.1(2)	53.1(3)
$O^2P^2O^1C^7$	175(2)	173.2(2)	174.9(2)	178.4(2)	177.7(3)
$O^3P^2O^1C^7$	46(2)	45.8(2)	46.2(3)	50.8(2)	51.3(3)
$O^1P^2O^3C^4$	44(2)	45.1(2)	43.3(3)	39.3(3)	38.5(3)
$O^2P^2O^3C^4$	80(2)	79.0(2)	82.1(3)	85.9(3)	86.4(3)
$O^4P^2O^3C^4$	153(2)	156.2(2)	153.0(3)	147.0(3)	146.5(3)
$P^2O^1C^7C^6$	67(3)	74.2(3)	72.8(4)	74.7(3)	70.4(4)
$P^2O^1C^7C^8$	110(2)	112.3(2)	112.0(3)	110.2(3)	116.2(3)
$P^2O^3C^4C^5$	65(2)	65.0(2)	59.4(4)	63.0(4)	67.9(4)
$O^3C^4C^5C^6$	5.25(3)	4.4(3)	12.9(5)	3.9(4)	5.8(5)
$O^3C^4C^5O^5$	176(2)	179.2(2)	168.9(3)	176.3(3)	171.8(4)
$C^4C^5C^6C^7$	52(4)	43.4(3)	52.5(5)	44.9(5)	39.5(6)
$O^5C^5C^6C^{11}$	36(3)	35.1(4)	45.4(5)	32.3(5)	31.5(6)
$O^5C^5C^6C^7$	129(3)	142.1(3)	129.4(4)	143.3(4)	143.1(5)
$C^5C^6C^7O^1$	6(4)	4.7(4)	0.3(5)	1.8(5)	1.1(6)
$C^5C^6C^7C^8$	177(3)	178.0(2)	175.1(4)	176.6(3)	171.8(4)
$C^{11}C^6C^7O^1$	172(2)	172.4(2)	174.4(3)	173.8(3)	175.5(3)
$C^{11}C^6C^7C^8$	11(4)	0.8(4)	0.5(6)	1.1(5)	2.7(6)
$O^1P^2O^4C^{12}$	112(2)	111.7(2)	111.3(3)	131.3(2)	152.9(3)
$O^2P^2O^4C^{12}$	14(2)	15.2(2)	15.1(3)	5.1(3)	26.2(3)
$O^3P^2O^4C^{12}$	142(2)	140.9(2)	141.0(3)	121.9(2)	99.9(3)
$P^2O^4C^{12}C^{13}$	136(2)	104.7(2)	130.6(3)	109.7(3)	76.5(3)
$P^2O^4C^{12}C^{14}$	–108(2)	–132.3(2)	–106.9(3)	–126.0(2)	–159.1(2)
Q[a]	0.883(21)	0.864(2)	0.894(3)	0.867(3)	0.843(3)

[a] *Q* is the Cremer–Pople heteroring puckering parameter [16].

"pseudoequatorial" and "pseudoaxial," since the unsymmetrical conformation of the ring leads to a situation when one and the same substituent has different conformations along endocyclic P–O bonds determining its position: *gauche* from one side (what corresponds to the axial position) and *transoid* from the other (what corresponds to the equatorial position). The principal torsion angles in the heterorings of molecules **VIII**–**XII** and angles describing substituent positions in them are listed in Table 3.

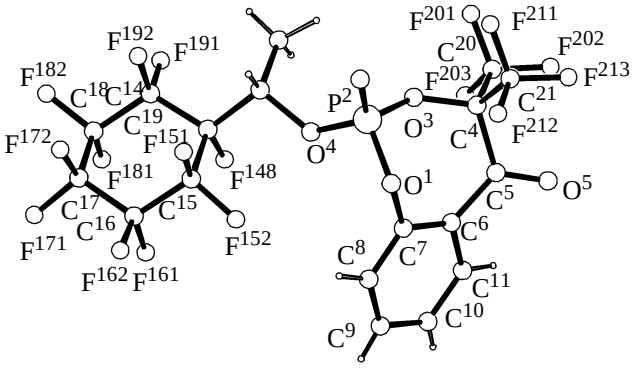

Fig. 5. Molecular geometry of phosphepine **XII** in crystal and numbering scheme.

We also examined heteroring puckering in these molecules according to Cremer and Pople [16]. As shown in Table 3, the torsion angles in the heterorings of compounds **VIII**–**XII** are no larger than 10°, and the puckering amplitudes also do not vary significantly. Nevertheless, it can be noted that the strongest heteroring puckering is characteristic of molecules **VIII** and **X**, and the most flattened heteroring is observed in molecule **XII** with the bulky perfluorocyclohexyl substituent. Hence, it can be proposed that bulky substituents on phosphorus lead to heteroring flattening. Since the heteroring conformations in previously studied molecules **XIII** and **XV** differ from those established for structures **VIII**–**XII**, we do not compared their puckering parameters. Therewith, the puckering amplitude of the heteroring in **XV** is slightly larger [1.033(3) Å] than in **VIII**–**XII** [average 0.923(3) Å]. Note that the C^4 atom in **XIII** and **XV** bears ethoxy- and methoxycarbonyl substituents. Consequently, the flattened unsymmetrical *twist-bath*

Table 4. Principal bond lengths *d* (Å) in molecules **VIII**–**XII** and **XV**

Bond	**VIII**	**IX**	**X**	**XI**	**XII**	**XV**[a]
P^2–O^1	1.55(2)	1.566(2)	1.564(3)	1.568(3)	1.567(2)	1.582(3)
P^2–O^2	1.45(1)	1.443(1)	1.438(2)	1.440(2)	1.448(3)	1.451(3)
P^2–O^3	1.59(2)	1.592(1)	1.586(2)	1.584(2)	1.600(3)	1.585(3)
P^2–O^4	1.58(2)	1.563(2)	1.560(2)	1.556(2)	1.549(2)	1.536(3)
O^1–C^7	1.45(3)	1.402(2)	1.430(4)	1.414(3)	1.420(4)	1.408(4)
O^3–C^4	1.48(3)	1.414(3)	1.427(4)	1.417(3)	1.408(5)	1.425(5)
O^4–C^{12}	1.43(3)	1.466(2)	1.449(4)	1.464(3)	1.467(4)	1.456(7)
O^5–C^5	1.29(3)	1.206(3)	1.220(5)	1.207(4)	1.185(6)	1.210(4)
C^4–C^5	1.49(4)	1.564(3)	1.548(6)	1.574(5)	1.573(5)	1.554(6)
C^5–C^6	1.45(3)	1.478(4)	1.487(5)	1.475(5)	1.486(4)	1.487(5)
C^6–C^7	1.34(3)	1.390(3)	1.372(5)	1.370(4)	1.361(6)	1.402(6)

[a] Average values for two independent molecules in the crystal are listed [10]

conformation of these heterorings is determined by the substituents on the C^4 atom. The fact that the heteroring conformation in six of the ten 1,3,2-dioxaphosphepines studied is distorted unsymmetrical *bath*, which is also true of the seven 1,4,2-dioxa- and oxazaphosphepines **XX**–**XXVI**, gives us grounds to state that this conformation is most characteristic of 6,7-benzo-1,3,2- and 6,7-benzo-1,4,2-oxaheterophosphepines.

As mentioned above, the phosphoryl group in **VIII**–**XII** occupies the pseudoequatorial position, and the alkoxy substituent is pseudoaxial. This complies with the anomeric effect and is best presented graphically by means of Newman projections. Below we give the Newman projects along the O–P bonds in molecule **XII**; in the other molecules, the general view of the projections is the same.

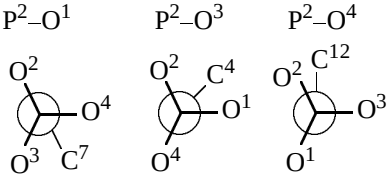

It is readily seen that the anomeric oxygen atom in these molecules has the usual chess conformation along the O^1–P^2 bond. This conformation favors hyperconjugation interactions between lone electron pairs of O^1 and nonbonding orbitals of the O^3–P and O^4–P bonds (n–σ^* interaction). At the same time, the conformation along the O^3–P bond is only favorable for interaction of its lone electron pairs with the antibonding orbital of the $P{=}O^2$ σ bond. Along the exocyclic P–O^4 bond, an eclipsed conformation with the P=O bond *cis* to O^4–P is formed, that is symmetrical in **XI** and slightly unsymmetrical in the other molecules (Table 3). In this conformation, n–σ^* interaction of lone electron pairs of the exocyclic oxygen atom with antibonding orbitals of one or two endocyclic O–P bonds (inverse anomeric effect) is possible. In molecule **XV**, the ethoxy group on phosphorus is pseudoequatorial and renders impossible n–σ^* interaction of lone electron pairs of O^1 with the exocyclic P–O bond.

The above reasoning generally agrees with the trends in bond lengths and angles at the phosphorus atom in molecules **VIII**–**XII** that have an axial alkoxy substituent, as well as in molecule **XV** that has an equatorial ethoxy group (Table 4 and 5). Regretfully, we have to exclude from this comparison structure **VIII** whose geometric parameters were determined with large experimental errors. As follows from Table 4, the endocyclic O^1–P^2 bonds in **VIII**–**XII** are shorter than in **XV**, while the endocyclic O^4–P bonds are longer. This difference in bond lengths can be explained by the anomeric effect in the former molecules and by the inverse anomeric effect in the latter. The same stereoelectronic effects may cause the difference in the endocyclic $O^1P^2O^3$ bond angles. In molecules **VIII**–**XII**, these angles are considerably larger [103.8(1)–104.7(1)°] than in molecule **XV** [on average, 102.7(1)°] (Table 5). Hence, the analysis of the geometric parameters of molecules **VIII**–**XII** shows that the observed trends in bond lengths and angles at the phosphorus atom are explainable in terms of the general anomeric effect, and that the model of hyperconjugation stereoelectronic interaction is feasible for interpreting the structure of such unsymmetrical heterocyclic systems.

The geometry of substituents in molecules **VIII**–**XII** is usual. In phosphepines **VIII**–**XI**, an eclipsed conformation with the P^2–O^4 bond shielding C^{12}–H is

Table 5. Principal bond angles ω (deg) in molecules **VIII**–**XII** and **XV**

Angle	VIII	IX	X	XI	XII
$O^1P^2O^2$	111(1)	111.98(9)	112.2(2)	113.2(1)	113.3(1)
$O^1P^2O^3$	104.1(9)	103.81(8)	104.7(1)	103.6(1)	103.8(1)
$O^1P^2O^4$	107.3(8)	108.3(1)	107.0(1)	104.6(1)	104.7(1)
$O^2P^2O^3$	118.3(9)	117.2(1)	117.7(1)	116.9(1)	115.8(1)
$O^2P^2O^4$	117.8(9)	116.17(9)	116.3(1)	117.1(1)	117.4(2)
$O^3P^2O^4$	96.6(8)	97.86(8)	97.2(1)	99.6(1)	99.9(1)
$P^2O^1C^7$	125(2)	122.3(1)	121.9(2)	120.5(2)	121.5(2)
$P^2O^3C^4$	127(1)	128.4(1)	129.0(2)	130.5(2)	129.9(2)
$P^2O^4C^{12}$	121(1)	121.1(1)	123.3(2)	123.8(2)	123.8(2)
$O^3C^4C^5$	110(2)	114.4(2)	114.1(3)	113.8(3)	113.2(2)
$O^5C^5C^4$	111(2)	116.2(2)	116.8(3)	115.6(3)	116.0(3)
$O^5C^5C^6$	122(3)	122.3(2)	122.2(4)	122.4(3)	122.2(4)
$C^4C^5C^6$	127(2)	121.3(2)	120.9(3)	121.6(3)	121.7(4)
$C^5C^6C^7$	124(2)	124.7(2)	123.8(3)	124.3(3)	126.4(4)
$C^5C^6C^{11}$	118(2)	117.9(2)	116.8(3)	117.7(3)	115.6(4)
$C^7C^6C^{11}$	116(2)	117.4(2)	119.2(3)	117.9(3)	117.7(3)
$O^1C^7C^6$	117(2)	119.8(2)	118.7(3)	117.9(3)	120.8(3)
$O^1C^7C^8$	117(2)	117.9(2)	117.5(3)	117.5(2)	116.2(4)

realized along the O^4–C^{12} bond. Therewith, the bulky fluorinated substituents are anticlinal with respect to the P^2–O^4 bond, thus best minimizing steric contacts in the molecule. Compound **XII** is an outlier of this series. It features a chess conformation along the P^2–O^4 bond with *transoid* location of the P^2–O^4 and C^{12}–C^{14} bonds. In such a conformation, the heteroring and bulky perfluorocyclohexyl substutuents are remote from each other as much as possible. Hence, the conformations along exocyclic P–O bonds in phosphepines **VIII**–**XII** are evidently controlled by steric factors.

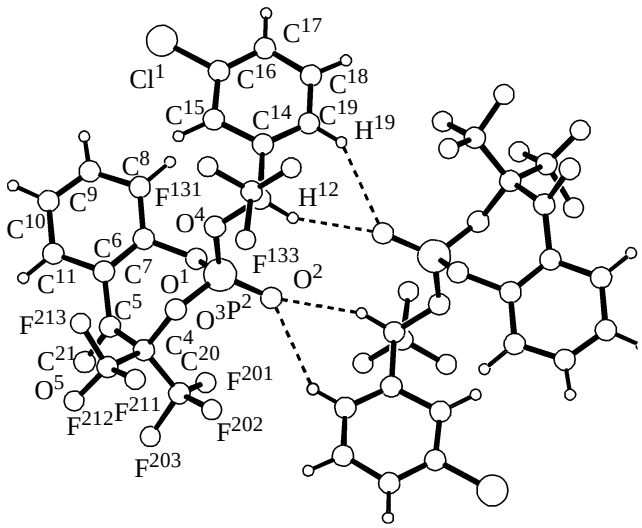

Fig. 6. Hydrogen-bonded dimer of molecule **VIII** in crystal. Hydrogen bonds are shown by dashed lines.

Having a sufficiently large set of similar structures, we could analyze and generalize the peculiarities of intra- and intermolecular interactions in compounds **VIII**–**XII** as a function of the type of the exocyclic substituent on phosphorus. The molecules have identical heterocyclic fragments and differ only in the nature of radicals on the chiral α-carbon atom (C^{12}) of the exocyclic alkoxy substituent. Nevertheless, as we showed above, the nature of the radical exerts a certain effect on the heteroring conformation (in particular, this is reflected in the varied heteroring puckering parameter).

Note that compounds **VIII**–**XII** all form crystals free of solvent molecules. Inspite of the absence of classical hydrogen bonds, these crystals contain a developed system of intermolecular interactions of other types, in detail C–H···O–, C–H···π– , and π–π. Moreover, many short contacts involving fluorine atoms are observed, which, too, can considerably affect the crystal packing [17].

The formation of hydrogen-bonded dimers is characteristic of all the compounds under study. Hence, the formation of a couple of bifurcate C–H···O hydrogen bonds between O^2 and the H^{12} and H^{19} protons of two molecules **VIII** related to each other by a symmetry center gives rise to dimer formation (Fig. 6). The C^{12}–H^{12}···O^2 (1 – *x*, –*y*, –*z*) and C^{19}–H^{19}···O^2

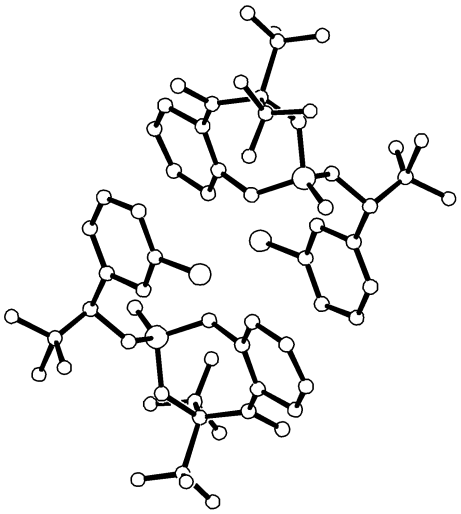

Fig. 7. π-Dimer of molecules **VIII** in crystal. Hydrogen atoms are not shown.

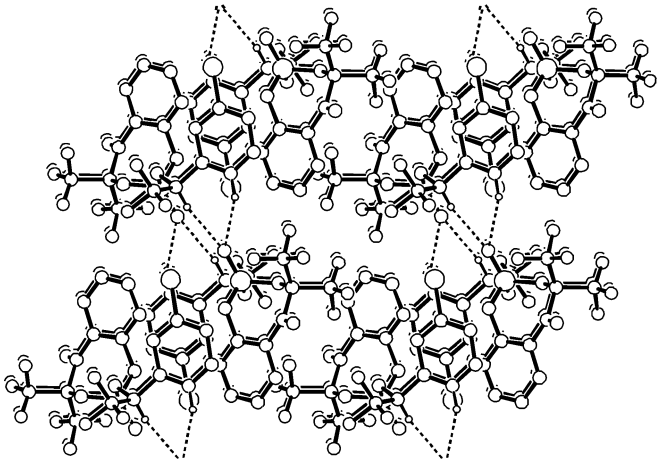

Fig. 8. Crystal packing of molecules **VIII** and formation of a bilayer structure. Hydrogen bonds are shown by dashed lines.

interaction parameters in the crystal of compound **VIII** are the following: C^{12}–H^{12} 0.99 Å, $H^{12}\cdots O^{2'}$ 2.37 Å, C^{12}–$H^{12}\cdots O^{2'}$ angle 159°C and C^{19}–H^{19} 0.99 Å, $H^{19}\cdots O^{2}$ 2.57 Å, C^{19}–$H^{19}\cdots O^{2}$ angle 144°, respectively.

In addition, O^2 forms an intramolecular contact with H^{12} ($H^{12}\cdots O^2$ 2.52 Å, C^{12}–$H^{12}\cdots O^2$ 110°). Thus O^2 takes part in a trifurcate hydrogen bond. The planes of the phenyl substituent and condensed benzene fragment are almost parallel to each other, the dihedral angle between them is 10.9°, and the distance between the ring centers is 5.65 Å. Despite the insignificant overlap of these planes the PLATON program [18] we used to analyze intra- and intermolecular interactions shows the presence of intramolecular π–π interactions between them. Note that the mutual location of the phehyl and benzo fragments in the molecule occurs to be favorable for their intermolecular contact with the π-systems of the phenyl and benzo fragments of a neighboring molecule related to the former by a symmetry center (*–x*, *–y*, *–z*), thus leading to formation of a peculiar molecular π-dimer (Fig. 8). Parameters of these contacts are identical, the dihedral angle between the ring planes is 10.9°, and the distance between the ring centers is 3.82 Å.

Therewith, the phenyl substituents of molecules related as (*–x*, 1 – *y*, *–z*) form a short contact (dihedral angle 0°, distance between the ring centers 3.71 Å), giving rise to the stacking effect between them. These interactions lead to formation of a dimeric layer of molecules, located parallel to the 0*xy* crystallographic plane (since the phenyl substituents of dimeric molecules enter stacking interaction with the phenyl rings of molecules from neighboring stacks) (Fig. 8).

Here we deal with an effect of localization of hydrophilic and hydrophobic regions in the crystal, resulting in formation of lamellar structures (layers comprising cyclic fragments and layers comprising organofluorine fragments, alternating along the 0*x* axis). Such location facilitates multiple F···F (average interatomic distance 3.07 Å) and Cl···F contacts. All the above-mentioned contacts lead to a tight crystal packing (packing factor 68.7%, specific gravity 1.77 g/cm^3) containing no free space. Hence, the formation of supramolecular lamellar motifs in the

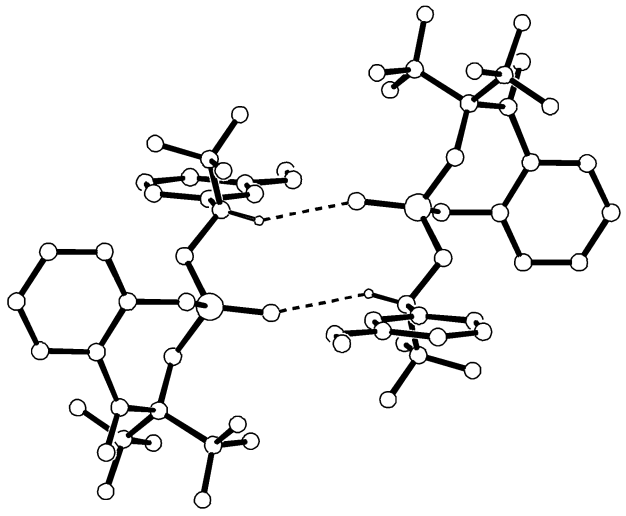

Fig. 9. Hydrogen-bonded dimer of molecules **IX** in crystal. Hydrogen bonds are shown by dotted lines.

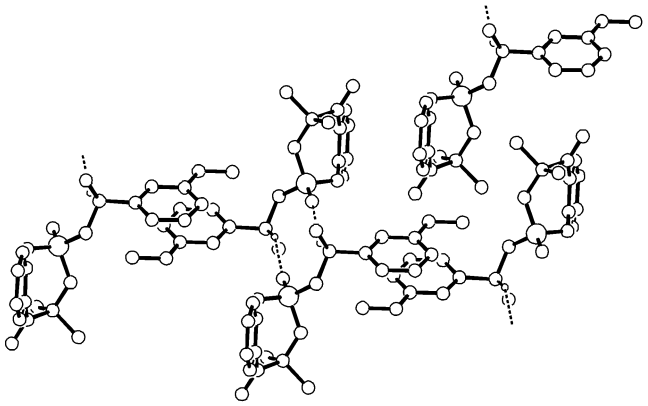

Fig. 10. π–π Interactions of molecules in the crystal of compound **IX**. Hydrogen atoms are not shown.

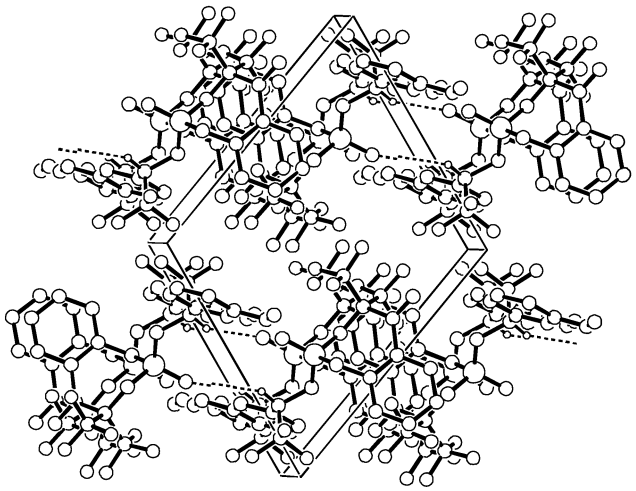

Fig. 11. Crystal packing of molecules **IX** and formation of a bilayer structure.

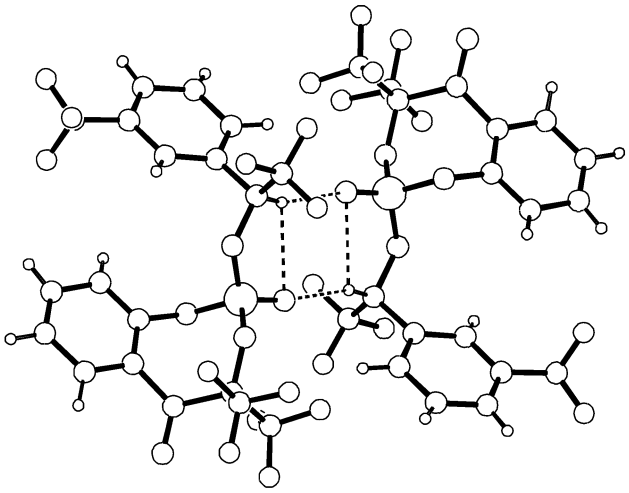

Fig. 12. Hydrogen-bonded dimer of molecules **X** in crystal. Hydrogen bonds are shown by dashed lines.

crystal of compound **VIII** is determined by various π–π, C–H···O, and C–H···F interactions that bind molecules along two mutually perpendicular directions. Note that the configuration of the chiral P^2 and C^{12} atoms in **VIII** is the same (S_P, S_C or R_P, R_C), because this product is racemic and crystallizes in a centrosymmetric group.

Substitution of chlorine in the phenyl fragment by a methoxy group in compound **IX** completely changes the molecular conformation, while not significantly affecting the heteroring conformation. First of all note that such substitution leads to crystallization of the other diastereomer (the configurations of P^2 and C^{12} do not coincide) in which the substituents on O^4 are rotated so that the benzo fragment is practically perpendicular to the phenyl plane [dihedral angle 86.1°] (Fig. 10). Such conformation leads to a looser crystal packing (packing factor 67.7%, specific gravity 1.65 g/cm^3), even though no free space available for solvents appears. As a result, molecular dimers are formed exclusively by two C–H···O bonds between H^{12} and $O^{2'}$ (1 – *x*, 1 – *y*, 2 – *z*), having the following parameters: $H^{12}\cdots O^{2'}$ 2.33(2) Å, C^{12}–$H^{12}\cdots O^{2'}$ angle 151.2(2)° (H^{19} is not involved in hydrogen bonding). The same atoms form an intramolecular $H^{12}\cdots O^2$ contact [$H^{12}\cdots O^2$ distance 2.44(2) Å, C^{12}–$H^{12}\cdots O^2$ angle 116(1)°].

Each of the molecules in a dimer takes part in two π–π contacts in mutually perpendicular directions (Fig. 10). Molecular dimers form chains running the 0*bc* diagonal, by means of π-π interactions of the benzo fragments of neighboring molecules related as (1 – *x*, –*y*, 1 – *z*) (distance between the ring centers 3.71 Å, dihedral angle 0°).

The involvement of phenyl groups in mutual contacts with the corresponding substituents of molecules related to the initial one as (–*x*, –*y*, 2 – *z*) and (–*x*, 1 – *y*, 2 – *z*) (the distances between the rings centers are 5.31 and 5.36 Å, respectively, the dihedral angles are 0°) leads to formation of a dimeric layer of hydrogen-bonded molecules. These layers are parallel to the main diagonal of the cell (0*bc*) and separated from one another by lipophilic regions comprising organofluorine fragments (Fig. 11).

Such a lamellar crystal packing of molecules **IX**, too, gives rise to multiple short contacts between fluorine atoms and proves to be sufficiently tight for the crystal to contain no free space.

Since the crystals of compounds **X** and **VIII** are isostructural, the molecular conformations in them are the same. But the substitution of the methoxy group in the phenyl substituent by trifluoromethyl radically

changes the type of supramolecular structure and crystal packing. Therewith, the packing factor (67%) decreases, but the calculated specific gravity (1.73 g/cm^3) of the crystal of compound **X** increases.

Like in the above-described system of hydrogen bonds in the crystal of compound **VIII**, the phosphoryl oxygen atom O^2 in **X** is involved in a trifurcate hydrogen bond with the H^{12} and H^{19} protons of a molecule related to the initial one as (2 – *x*, –*y*, –*z*) and with the own H^{12} proton to form a hydrogen-bonded dimer (Fig. 12).

Note also that the substitution of the chlorine atom in the phenyl substituent of compound **VIII** by a trifluoromethyl group leads to a considerable weakening of intermolecular contacts in the crystal of compound **X**. The distances $H^{12}\cdots O^{2'}$ and $H^{19}\cdots O^{2'}$ vary from 2.37(2) Å and 2.57(2) Å in the former crystal to 2.60(2) Å and 2.71(4) Å in the latter. At the same time, the parameters of intramolecular interactions remain almost unchanged.

Analysis of the supramolecular structure of compound **X** reveals existence of supramolecular isomerism in its crystals [19]. From the viewpoint of intermolecular interactions [2], the supramolecular structure can be considered as a bilayer that comprises molecular dimers bound with each other in two mutually perpendicular directions by π–π contacts of aromatic rings and located in the 0*ab* plane. But from the viewpoint of separation of hydrophilic and hydrophobic regions, the supramolecular fragments can be considered as cylinders located along the 0*a* axis, with an inner hydrophilic and an outer hydrophobic regions (formed largely by fluorine atoms) (Fig. 14), unlike the lamellar crystal structure of **VIII**. As follows from the calculated degrees of hydrophilicity of the molecular fragments of compound **X**, the outer part of the condensed benzene ring, too, possesses hydrophobic properties. On the whole the crystal packing in this case can be regarded as parallel stacking of cylindrical fragments. Therewith, joining the hydro-

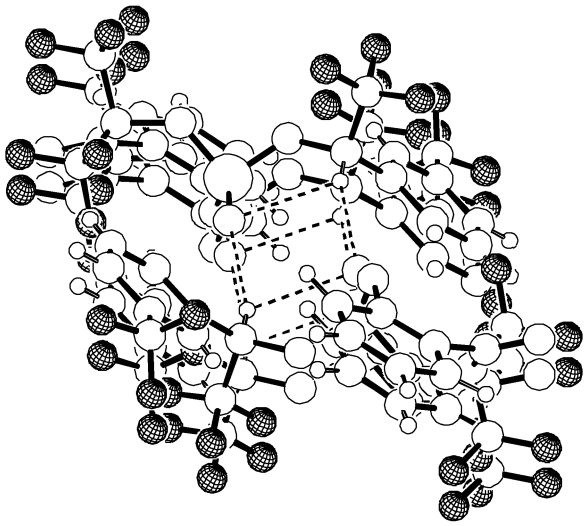

Fig. 13. Cylindrical supramolecular fragments in the crystal of compound **X**. Fluorine atoms are shadowed.

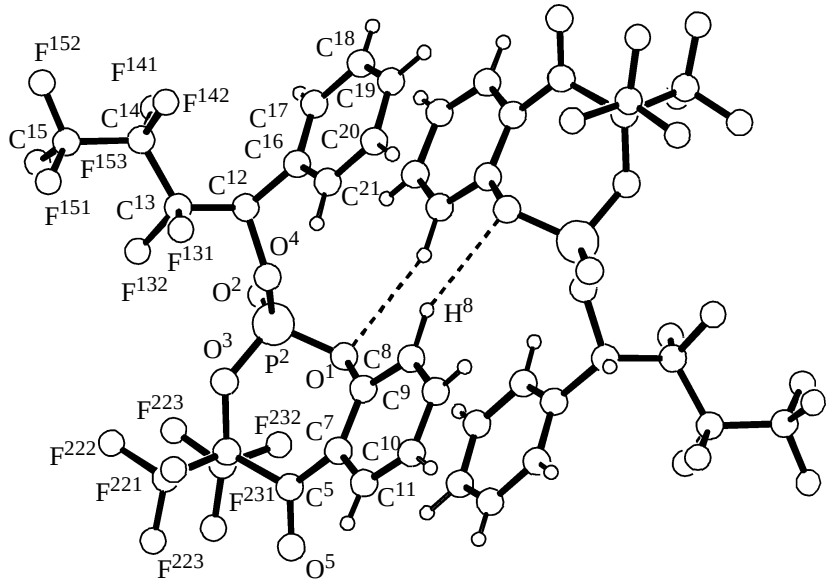

Fig. 14. Molecular dimer in the crystal of compound **XI**. Hydrogen bonds are shown by dashed lines.

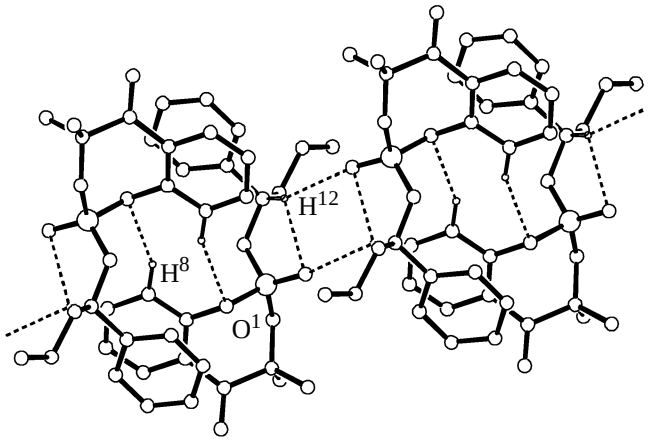

Fig. 15. Infinite chain of hydrogen-bonded molecules in the crystal of compound **XI**. Fluorine and hydrogen atoms of the benzo fragment are not shown.

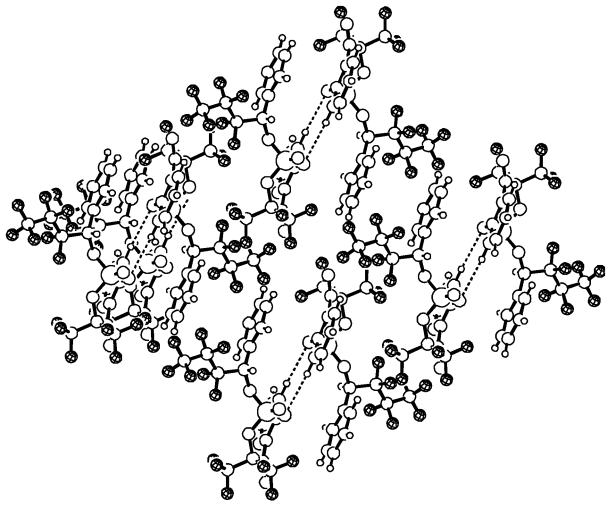

Fig. 16. Bilayer structure in the crystal of phosphepine **XI**. Fluorine atoms are shadowed.

phobic outer shells of the cylinders gives rise to multiple F···F and F···H contacts.

The crystals of **XI** are also isostructural to the crystals of **VIII** and **X**, the conformation of molecule **XI** is the same as of the above-mentioned compounds. Note that substitution of hexafluoropropyl trifluoromethyl on the chiral carbon atom C^{12} increases the calculated specific gravity (1.79 g/cm^3) and packing factor (67.9%). The dihedral angle between the phenyl and benzo ring planes is 0°, that is these planes are parallel. Such a mutual location is stabilized by an intramolecular hydrogen bond between O^4 and H^{21} [$H^{21}\cdots O^4$ distance 2.60(3) Å, C^{21}–$H^{21}\cdots O^4$ angle 152(7)°]. In the crystal of compound **XI**, centrosymmetric dimers are also formed by C–H···O interactions (Fig. 14), but the significant difference is that each molecule forms two dimers. One of them is formed by contacts between the H^8 and $O^{1'}$ (1 – *x*, –*y*, –*z*) atoms of neighboring molecules [$H^8\cdots O^{1'}$ distance 2.59(3) Å, C^8–$H^8\cdots O^1$ angle 156(3)°]. At the same time, pair π–π interaction is observed between the corresponding phenyl and condensed benzo fragments of the same molecules. The distance between the ring centers is 3.88 Å, and the dihedral angle is 3.58(2)°. Hence, this molecular dimer is formed both by hydrogen bonding and by interaction of aromatic fragments of the molecules. In their turn, the molecules of the dimer both form with neighboring molecules located along the 0*a* crystal axis a pair of identical contacts between H^{12} and O^2 [$H^{12}\cdots O^2$ distance 2.76 (3) Å, C^{12}–$H^{12}\cdots O^2$ angle 172.0(5)°], thus forming an infinite chain of hydrogen-bonded molecules (Fig. 15).

The molecules in these chains take part in π–π contacts with molecules of neighboring parallel chains to form tilted stacks of aromatic fragments with the shortest interplanar spacing of 3.66 Å and the dihedral angle of 0°. Under these conditions, the stacking effect takes place and formation of a two-dimensional bilayer supramolecular structure (Fig. 16) with in-layer localization of the fluorine-containing fragments. In terms of the model considering intermolecular interactions of only one type or our model considering separation of hydrophilic and hydrophobic regions in crystal, the most preferable in this case must be again a cylindrical supramolecular fragment with the inner part comprising hydrogen-bonded heterocyclic fragments and the outer part comprising the hydrophobic fluorine-containing radicals. Evidence for such a supramolecular block comes at least for the calculated degree of hydrophilicity of this molecule.

In the crystal of perfluorocyclohexyl derivative **XII**, maximum calculated specific gravity (1.95 g/cm^3) and packing factor (69%) are achieved. The same diastereomer as in most other cases (S_PS_C) crystallizes. At the same time, the crystal of **XII** is not isostructural to the crystals of **VIII**–**XI**. The mean plane of the cyclohexane ring occurs to be almost perpendicular to the plane of the benzo fragment [dihedral angle 77.0(2)°], like in a single analogous case of compound **IX**. The crystal of compound **XII** contains molecular contacts of various types (C–H···O, C–H···π, π–π, F···F and F···H). Therewith, only two C–H···O hydrogen bonds were found: an intramolecular contact $H^{12}\cdots O^{2'}$ and an intermolecular hydrogen bond $H^{12}\cdots O^{2'}$ (1 – *x*, 1 – *y*, –*z*) [$H^{12}\cdots O^{2'}$ distance 2.40(3) Å,

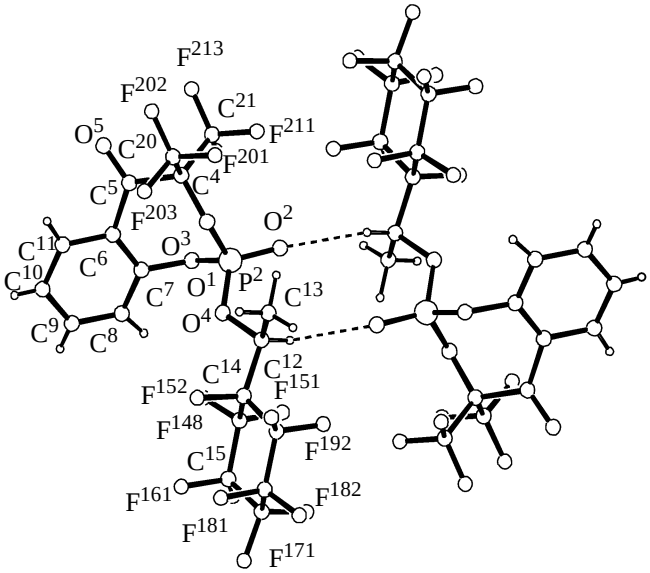

Fig. 17. Molecular dimer in the crystal of compound **XII**. Hydrogen bonds are shown by dashed lines.

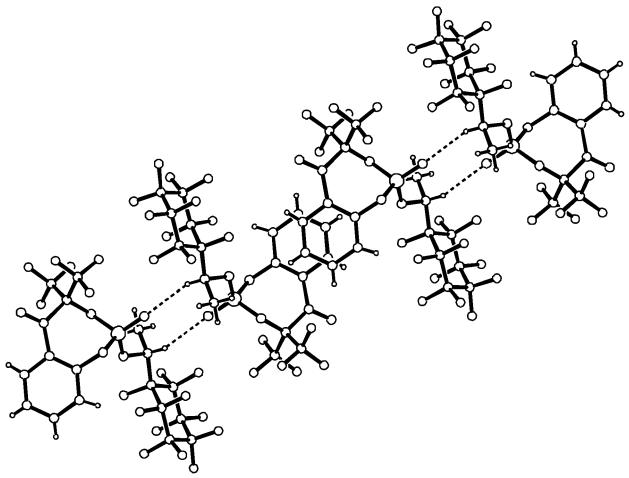

Fig. 18. Formation of a molecular chain in the crystal of compound **XII**.

C^{12}–$H^{12}\cdots O^{2'}$ angle 150(3)°], that lead to formation of a molecular dimer (Fig. 17).

The molecular dimers are bound with each other by π–π interaction of the condensed benzene rings to form a chain of dimers along the 0*c* axis (Fig. 18).

The molecular chains are located one above another in such a way that the parallel packing of such supramolecular fragments gives rise to the stacking effect, viz. π–π interactions between the condensed benzo substituent of each molecule and the benzo fragments of two other molecules related to the initial one by a symmetry center and translations by +1 and –1 along the 0*a* axis (distance between the ring centers 3.66 and 4.05 Å, dihedral angle 0°). The shortest interplanar spacing is 3.51 Å. Thus a two-dimensional lamellar structure is formed. The intermolecular interactions in two directions inside the layer differ in nature. Along the 0*c* axis, C–H···O and π–π contacts take place, while along the 0*a* axis, π–π contacts exclusively. Allowance for only one of the revealed types of interactions, for example, contacts between aromatic systems, would result in a cylindrical supramolecular structure.

Here, again, we observe localization of hydrophilic and hydrophobic regions in the crystal, because the above-described layers alternate along the 0*b* axis with layers comprising fluorine-containing substituents (Fig. 19).

The above analysis of the structure of the compounds and their crystal packing allows certain conclusions. The compounds all crystallize in triclinic centrosymmetric cells with fairly close parameters, but only three crystals among the five considered are isostructural. In most compounds under study, the S_PS_C (R_PR_C) diastereomer with coplanar aromatic fragments crystallizes. Evidently, coplanarity of the aromatic fragments depends on the size of the substituent in the phenyl ring.

Intermolecular contacts in the crystals of all the compounds studied result in initial formation of molecular dimers. Evidently, it is a molecular dimer

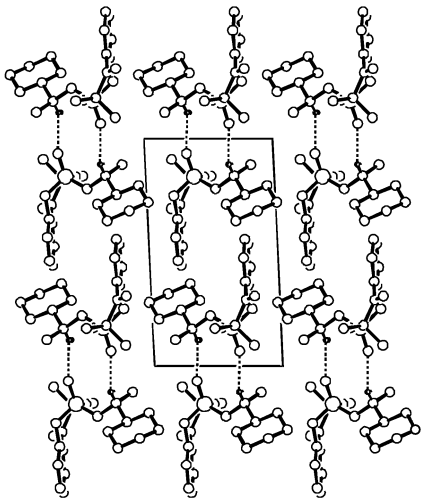

Fig. 19. Crystal packing of molecules **XII**. Hydrogen atoms are not shown.

that is a real supramolecular synthon [20] for this type of compounds. But there are different ways of binding of the dimers into supramolecular motifs: C–H···O contacts exclusively, combination of C–H···O and π–π contacts, or π–π contacts of two types. Contacts like F···F and F···H are observed in all the compounds. Their variability and specific features need separate consideration which is proposed to be made later with a broader range of compounds of this class.

The combined effect of intermolecular contacts gives rise to lamellar and cylindrical supramolecular structures. The isostructural crystals feature the effect of supramolecular isomerism: Depending on the chosen individual type of intermolecular contacts, supramolecular fragments of different topologies can be recognized in the crystals. Therewith, localization of regions containing fluorine-substituted fragments takes place. In view of the fact that the phosphorus-containing heterocyclic fragment is identical in all the compounds under study and all distinctions relate to the type of substituents on the O^4 atom, we can state that increasing number of fluorine atoms in a molecule (with the associated increase in the molecular weight) leads to increase in the specific gravity and the packing factor of its crystal.

Localization of fluorine-substituted fragments in the crystals is a specific case of the general phenomenon we revealed and described previously [21], that is separation of hydrophilic and hydrophobic regions in crystals. These regions not necessarily include the whole molecules of a compound or, for example, solvation molecules, and are formed by molecular fragments that possess largely hydrophilic or lipophilic properties. Our calculations of the degrees of hydrophilicity and hydrophobicity of the molecular fragments of the compounds in study and compounds of other classes, as well as comparison of the resulting values with the character of crystal packing provides unambiguous evidence for a more general character of this phenomenon. The associates formed as a result of such localization, which can be regarded as supramolecular structure, can assume the form of cylinders, layers and spheres similar to those observed in super crystals [22]. In particular, the crystal structures in study comprise cylindrical fragments with a hydrophilic inner and a hydrophobic outer (formed mainly by fluorine atoms) regions. The crystal packing in this case can be regarded as parallel packing of such cylindrical fragments, that joins the hydrophobic outer shells of the cylinders. Sometimes such supramolecular structures coincide with structural fragments formed by hydrogen bonding, but, evidently, this is not a general rule. Considering this fact provides a clearer understanding of the existence of supramolecular isomerism.

A possible reason for the amphiphilicity of molecules in crystals is their tendency for an energy minimum and, as a result, to leveling of the chemical potential inside the crystal, which is associated with the tendency for the largest possible interface between regions of different types. Therewith, however, constraints imposed by the symmetry of the crystals formed must be followed. Probably, lamellar structures in cubic crystals are impossible to form not disturbing the symmetry inherent in to this syngony. Note that weak interactions in the crystals of these compounds are not the main motive force of crystallization. Despite the fact that a number of compounds of the series in hand are isostructural, i.e. have similar crystal packings, the system of intermolecular contacts in the crystals can considerably vary, thus leading to different supramolecular structures. However, the separation of regions with largely hydrophilic and largely lipophilic properties is characteristic of all the compounds.

It is known from published data that four-coordinate phosporus derivatives containing residues of fluorinated secondary and tertiary alkanols structurally similar to those studied in the present work undergo a solid-phase diastereomeric transformation on prolonged handling [25]. We observed no such transformation in phosphepines **VII**–**XII** handled for 2 years at 20–25°C in sealed ampules.

EXPERIMENTAL

The IR spectra were recorded on a Specord IR-75 spectrometer in thin layer or suspensions in mineral oil between KBr plates. The NMR spectra were recorded on Bruker MSL-400 (^{13}C, 100.6 MHz; ^{31}P, 162 MHz), Varian Unity-300 (^{1}H, 300 MHz, ^{19}F, 282 MHz; ^{31}P, 121.4 MHz), and Bruker WP-200SY (^{19}F–$\{^{1}H\}$, 188.3 MHz) instruments.

Single-crystal X-ray diffraction analysis of compounds **VIII**–**XII** were carried out on an Enraft-Nonius CAD-4 automatic four-circle diffractometer (MoK_α or CuK_α radiation, graphite monochromator, $\omega/2\theta$ scanning, scan rate 1–16.4 deg/min by θ. Crystal stability was controlled by three control reflections measured every 2 h and crystal orientation, by two control reflexes centered every 200 measurements. No intensity decay of the control reflections was observed. The structure was solved by the direct method using the SIR program. Data processing and structure refinement were carried out using the MolEN program package on an AlphaStation 200 [24]. The refinement

Table 6. Parameters of the crystals of compounds **VIII**–**XII** and conditions of the X-ray diffraction experiments

Parameter	**VIII**	**IX**	**X**	**XI**	**XII**
Color, habitus	colorless needles	colorless prisms			
Unit cell parameters					
a, Å	9.26(1)	9.905(4)	9.308(6)	9.314(2)	7.180(2)
b, Å	10.657(6)	10.499(5)	10.902(4)	11.462(2)	12.259(3)
c, Å	11.054(7)	11.946(3)	11.56(1)	11.394(3)	14.119(3)
α, deg	80.45(5)	106.86(3)	77.33(3)	74.54(2)	64.60(2)
β, deg	76.77(8)	110.82(3)	75.11(5)	80.99(2)	86.33(2)
γ, deg	74.57(8)	99.87(3)	75.16(5)	75.43(2)	86.75(2)
Volume, A^3	1017(2)	1057.6(8)	1081(2)	1129.4(2)	1119.7(5)
Molecular weight	542.68	526.25	564.22	608.25	658.21
Specific gravity					
d_{calc}, g/cm^3	1.773	1.652	1.733	1.788	1.952
Absorption coefficient μ, cm^{-1}	3.718	22.286	24.051	2.526	2.865
F(000)	540	528	560	604	324
Radiation (λ, Å)	MoK_α λ 0.71073	CuK_α λ 1.54184		MoK_α λ 0.71073	
θ range	2.12 ≤ θ ≤ 27.4	4.2 ≤ θ ≤ 78.4		2.12 ≤ θ ≤ 27.4	
Scan angle	0.68 + 0.4tanθ	1.2 + 0.35tanθ		0.68 + 0.4tanθ	
Standard reflexes	Two control by orientation and three control by intensity every 200 reflections				
Index range	0 ≤ *h* ≤ 10 –11 ≤ *k* ≤ 11 –11 ≤ *l* ≤ 12	–10 ≤ *h* ≤ 9 –11 ≤ *k* ≤ 0 –12 ≤ *l* ≤ 13	0 ≤ *h* ≤ 9 –11 ≤ *k* ≤ 10 –22 ≤ *l* ≤ 22	–10 ≤ *h* ≤ 0 –12 ≤ *k* ≤ 12 –14 ≤ *l* ≤ 11	–8 ≤ *h* ≤ 8 –15 ≤ *k* ≤ 13 –17 ≤ *l* ≤ 0
Reflections measured	2935	2875	5044	3181	4294
Reflections with $I > 3\sigma(I)$	509	2600	2692	1998	2839
Allowance for absorption	not applied	empirical		not applied	
Conditions of location and refinement of hydrogen atoms	Revealed from the difference series, not refined	Revealed from the difference series, refined isotropically			Revealed from the difference series, not refined
Final divergence factors					
R	0.086	0.038	0.048	0.036	0.056
R_W	0.091	0.055	0.066	0.044	0.064
Fitting parameter	2.276	2.242	2.659	1.520	2.170
Δ/σ	0.00	0.02	0.01	0.00	0.00
Reflections refined	713	2520	1954	2055	2521
Parameters refined	147	364	370	392	370

[a] Triclinic syngony, space group *P*-1 (*P*1bar), *Z* = 2.

was carried out by the full-matrix least-squares procedure, the minimized function was $\Sigma w(|F_O| - |F_C|)^2$, extinction was not considered. The weight scheme was $4F_o^2/[\sigma(I)^2 + (0.04F_o^2)]^2$. The cell parameters and details of data collection and refinement of structures **VIII**–**XII** are given in Table 6. All drawings and analysis of intermolecular interactions were carried out by means of the PLATON program [18]. The principal geometric parameters are listed in Tables 2–5.

Fluoroalkoxy-5,6-benzo-1,3,2-dioxaphosphorinan-4-ones I–VI. To a solution of 0.05 mol of 2-chloro-5,6-benzo-1,3,2-dioxaphosphorinan-4-one in 100 ml of anhydrous ether, a solutiuon of 0.05 mol of fluorinated alcohol and triethylamine was added

dropwise with stirring at –30°C. The reaction mixture was stirred for 3 h until it achieved 20°C. The precipitate was filtered off, and the solvent was removed. The residue was dried in a vacuum (0.02 mm Hg) and then distilled. Phosphites **I**–**VI** were obtained as viscous colorless oils.

2-(2,2,2-trifluoro-1-phenylethoxy)-5,6-benzo-1,3,2-dioxophosphorinan-4-one (I). Yield 65%, bp 128°C (0.02 mm Hg), mp 62–64°C. IR spectrum, ν, cm^{-1}: 2900, 1730, 1600, 1580, 1455–1460, 1375, 1350, 1280–1290, 1230, 1202, 1170–1180, 1100–1130, 1040–1045, 960–980, 905–912, 890, 880, 850, 820, 780, 740–750, 700, 670. ^1H NMR spectrum (300 MHz, CCl_4 + 50% acetone-d_6), δ, ppm, (*J*, Hz): 6.85, 7.09, 7.18, 7.41, 7.52, 7.60–7.70, 8.18 all m (C_6H_4, C_6H_5, 9H), 5.90 q.d and 5.91 q.d (POCH, $^3J_{HCCF}$ 6.6, $^3J_{POCH}$ 8.7–9.0, 1H). ^{31}P–{^1H} (121.42 MHz, acetone-d_6) δ_P, ppm (*J*, Hz): 126.59 q ($^4J_{POCCF}$ 4.4, d_1); 124.26 q ($^4J_{POCCF}$ 4.4, d_2); d_1:d_2 52.4:47.6. ^{19}F NMR spectrum, δ_F, ppm (*J*, Hz): –75.16 m ($^3J_{HCCF}$ 6.6, $^4J_{POCCF}$ 4.5, d_1); –75.24 m ($^3J_{HCCF}$ 6.2; J_{POCCF} 4.5, d_2). Found, %: C 52.40; H 2.70. $C_{15}H_{10}F_3O_4P$. Calculated, %: C 52.63; H 2.92.

2-[1-(3-Chlorophenyl)-2,2,2-trifluoroethoxy]-5,6-benzo-1,3,2-dioxaphosphorinan-4-one (II). Yield 62%, bp 136–138°C (0.02 mm Hg). IR spectrum, ν, cm^{-1}: 3040, 1750, 1680, 1600, 1575, 1470, 1450, 1425, 1350, 1260–1285, 1175–1225, 1130, 1100–1110, 1025¨050, 1000–1010, 950, 895, 825–850, 805, 780, 745, 710, 680. ^{13}P–{^1H) NMR spectrum (121.42 MHz, 1:1 CCl_4:acetone-d_6), δ_P, ppm (*J*, Hz): 125.6 q ($^4J_{POCCF}$ 4.5, d_1); 123.17 q (J_{POCF} 4.5, d_2); d_1:d_2 50.2; 48.8. ^{19}F NMR spectrum, δ_F, ppm (*J*, Hz): –74.75 m ($^4J_{POCCF}$ 4.5, $^3J_{FCCH}$ 4.6, d_1); –74.82 m ($^4J_{POCCF}$ 4.5, $^3J_{FCCH}$ 4.6, d_2). Found, %: C 47.60; H 2.40. $C_{15}H_9 \cdot ClF_3O_4P$. Calculated, %: C 47.80; H 2.39.

2-[2,2,2-Trifluoro-1-(3-methoxyphenyl)ethoxy]-5,6-benzo-1,3,2-dioxaphosphrinan-4-one (III). Yield 58%, bp 152–154°C (0.02 mm Hg). IR spectrum, ν, cm^{-1}: 3080, 2940, 1750, 1690, 1600, 1580, 1485, 1460, 1430, 1350, 1280, 1260, 1170, 1130, 1030, 1000, 930, 900, 860, 840, 820, 775, 750, 700, 680. ^{31}P–{^1H} NMR spectrum (121.42 MHz, acetone-d_6), δ_P, ppm: 123.25 br.s (d_1), d_2 121.82 br.s (d_2); d_1; d_2 51:49. Found, %: C 51.40; H 3.54. $C_{16}H_{12}F_3O_5P$. Calculated, %: C 51.61; H 3.23.

2-[2,2,2-Trifluoro-1-(3-trifluoromethylphenyl)-ethoxy]-5,6-benzo-1,3,2-dioxaphosphorinan-4-one (IV). Yield 60%, bp 126–128°C (0.02 mm Hg), mp 68–70°C. IR spectrum, ν, cm^{-1}: 2920, 2860, 1745, 1655, 1600, 1570, 1340–1345 sh., 1330, 1280, 1255, 1220, 1150–1180, 1120, 1090, 1050–1060, 1030, 1000, 970–980, 910, 890, 870, 860, 820, 790, 780, 740, 700, 680. ^{31}P–{^1H} (121.42 MHz, acetone-d_6), δ_P, ppm (*J*, Hz): 126.59 q ($^4J_{POCCF}$ 4.5, d_1); 124.26 q ($^4J_{POCCF}$ 4.5, d_2); d_1:d_2 52.4:47.6. ^{19}F NMR spectrum, δ_F, ppm (*J*, Hz): d_1 –60.51 br.m (CF_3), –75.48 m ($^4J_{POCCF}$ 4.5, $^3J_{FCCH}$ 4.6, d_1); –60.55 br.s (CF_3), –75.39 m ($^4J_{POCCF}$ 4.5, $^3J_{FCCH}$ 4.6, d_2). Found, %: C 47.05; H 2.61. $C_{16}H_9F_6O_4P$. Calculated, %: C 46.83; H 2.20.

2-(2,2,3,3,4,4,4-heptafluoro-1-phenylbutoxy)-5,6-benzo-1,3,2-dioxaphosphorinan-4-one (V). Yield 65%, bp 124–128°C (0.02 mm Hg), mp 67–70°C. IR spectrum, ν, cm^{-1}: 3060, 2860, 1750, 1680, 1600, 1675, 1535, 1470, 1455, 1390, 1335, 1280, 1200–1230, 1165–1180, 1140, 1100, 1075, 1010, 995, 960, 940, 900, 860, 840, 745 sh, 740, 715, 685, 640. ^{31}P–{^1H} NMR spectrum (121.42 MHz, 1:1 CCl_4–acetone-d_6), δ_P, ppm: 125.88 br.s (d_1), 123.98 br.s (d_2), d_1:d_2 50.5:49.5. ^{19}F NMR spectrum (acetone-d_6), δ_F, ppm (*J*, Hz): –78.91 d.d (CF_3, $^3J_{F_ACCF}$ 9.0, $^3J_{F_BCCF}$ 12.1, d_1); –79.03 d.d (CF_3, $^3J_{F_ACCF}$ 9.0, $^3J_{F_BCCF}$ 12.0, d_2), –123.5–123.8 m (CF_2CF_2, d_1, d_2). Found, %: C 46.40; H2.62. $C_{17}H_{10}F_7O_4P$. Calculated, %: C 46.15; H 2.26.

2-[1-Methyl-1-(perfluorocyclohexyl)ethoxy]-5,6-benzo-1,3,2-dioxaphosphorinan-4-one (VI). Yield 71%, bp 99–100°C (0.02 mm Hg). IR spectrum, ν, cm^{-1}: 3100, 2960, 1760, 1610, 1570, 1460, 1330, 1280, 1240, 1180, 1120, 1090, 1060, 1030, 1000, 970, 910, 890, 870, 860, 820, 790, 780, 760, 740, 700, 680. ^{31}P–{^1H} NMR spectrum (121.42 MHz, acetone-d_6), δ_P, ppm: 125.65 br.s (d_1), 124.49 br.s (d_2), d_1:d_2 1:1. Found, %: C 36.70; H 1.81. $C_{15}H_8F_{11}O_4P$. Calculated, %: C 36.58; H 1.63.

Reaction of phosphorinanes I–VI with hexafluoroacetone *(general procedure).* A solution of 0.01–

0.015 mol of phosphorinane **I**–**VI** in 30 ml of CH_2Cl_2 was treated at –40°C with 0.015–0.02 mol of hexafluoroacetone under argon. The reaction mixture was gradually (2–3 h) heated to 20°C. After a day, the solvent and excess hexafluoroacetone were removed. The residue was phosphepine **VII**–**XII** (colorless viscous oil), quantitative yield. It was a mixture of diastereomers in a ratio similar to that in the starting phosphite. The oil was dissolved in a mixture of 10–20 ml of methylene chloride and diethyl ether and left to stand for 10–20 days at 0–5°C. Crystals of individual diastereomers precipitated (yield 37–43%) and were filtered off, washed with a cold mixture of methylene chloride and pentane, and dried in a vacuum (12 mm Hg). The crystals used for X-ray studies were recrystallized from acetone.

4,4-Bis(trifluoromethyl)-2-(2,2,2-trifluoro-1-phenylethoxy)-6,7-benzo-1,3,2λ^5-dioxaphosphepin-5-one 2-oxide (VII) *Diastereomeric mixture.* ^{31}P–$\{^1H\}$ NMR spectrum (162.0 MHz, CCl_4), δ_P, ppm: 115.32 s and –15.55 s. *Isolated diastereomer.* mp 115–124°C. IR spectrum, cm^{-1}: 2940, 2860, 1720, 1600, 1330, 1265–1275, 1240–1250, 1210, 1180, 1130, 1110, 1075, 1050, 975, 930, 920, 885, 790, 775, 750, 740, 700, 680, 660, 630, 610, 590, 550, 570, 550, 525, 490, 460. ^{31}P–$\{^1H\}$ NMR spectrum (162.0 MHz, CCl_4):δ_P –15.35 ppm. Found, %: C 42.40; H 1.86. $C_{18}H_{10}F_9O_5P$. Calculated, %: C 42.52; H 1.97.

4,4-Bis(trifluoromethyl)-2-[1-(3-Chlorophenyl)-2,2,2-trifluoroethoxy]-6,7-benzo-1,3,2λ^5-dioxaphosphepin-5-one 2-oxide (VIII). *Diastereomeric mixture.* ^{31}P–$\{^1H\}$ NMR spectrum (162.0 MHz, CCl_4), δ_P, ppm: –15.76 s and –16.06 s. *Isolated diastereomer*: mp 143–145°C. IR spectrum, ν, cm^{-1}: 2930, 1730, 1700, 1610, 1590, 1320, 1275, 1250, 1220, 1195, 1170, 1145, 1100, 1050, 975, 965, 935, 920, 890, 850, 785, 770, 745, 730, 715, 700, 665, 650, 630, 615, 585, 550, 525, 510, 480, 440. ^{31}P–$\{^1H\}$ NMR spectrum (162.0 MHz, CCl_4): δ_P –15.76 ppm. Found, %: C 39.86, H 1.81. $C_{18}H_9ClF_9O_5P$. Calculated, %: C 39.82, H 1.66.

4,4-Bis(trifluoromethyl)-2-[2,2,2-trifluoro-1-(3-methoxyphenyl)ethoxy]-6,7-benzo-1,3,2λ^5-dioxaphosphepin-5-one 2-oxide (IX). *Diastereomeric mixture.* IR spectrum, ν, cm^{-1}: 3080, 2980, 2940, 1795, 1725, 1700, 1650, 1615, 1600 sh, 1570 sh, 1560, 1525, 1500, 1465, 1445, 1370–1380, 1320, 1300, 1280, 1220–1260, 1200, 1190, 1140, 1120, 1060, 1040, 980, 950, 918 sh, 885, 850, 790, 770 sh, 715, 690, 670, 650, 640, 600, 565, 530, 510, 490, 465, 430. ^{31}P–$\{^1H\}$ NMR spectrum (162.0 MHz, CCl_4), δ_P, ppm: –15.7 s and –15.8 s. *Isolated diastereomer.* mp 121–125°C. ^{31}P–$\{^1H\}$ NMR spectrum (162.0 MHz, CCl_4): δ_P –15.0 ppm. ^{19}F–$\{^1H\}$ NMR spectrum (188.3 MHz, acetone-d_6), δ_F, ppm (*J*, Hz): –69.3 q and –70.81 q [$C(CF_3)_2$, $^4J_{FCCCF}$ 9.3], –75.14 s (CHF_3). Found, %: C 42.40; H 1.86. $C_{19}H_{12}F_9O_6P$. Calculated, %: C 42.38; H 2.23.

4,4-Bis(trifluoromethyl)-2-[2,2,2-trifluoro-1-(3-trifluoromethylphenyl)ethoxy]-6,7-benzo-1,3,2λ^5-dioxaphosphepin-5-one 2-oxide (X). *Diastereomeric mixture.* $^{31}P\{^1H\}$ NMR spectrum (162.0 MHz, CCl_4), δ_P, ppm: –16.9 s and –16.2 s. *Isolated diastereomer.* mp 87–90°C. IR spectrum, ν, cm^{-1}: 2940, 2870, 1720, 1605, 1575, 1540, 1520, 1455, 1330, 1320, 1267, 1240, 1220, 1190, 1155, 1125, 1110, 1075, 1050, 980, 960, 930, 890, 850, 805, 790, 770, 740, 710, 660, 630, 625 sh, 615, 590, 570, 550, 525, 510, 480, 411. ^{31}P–$\{^1H\}$ NMR spectrum (CCl_4): δ_P –16.12 ppm. Found, %: C 39.40; H 1.86. $C_{19}H_9F_{12}O_6P$. Calculated, %: C 39.58; H 1.56.

4,4-Bis(trifluoromethyl)-2-(2,2,3,3,4,4,4-heptafluoro-1-phenylbutoxy)-6,7-benzo-1,3,2λ^5-dioxaphosphepin-5-one 2-oxide (XI). *Diastereomeric mixture.* ^{31}P–$\{^1H\}$ NMR spectrum (162.0 MHz, CCl_4), δ_P, ppm: –15.71 s and –16.2 s. *Isolated diastereomer.* mp 122–124°C. IR spectrum, ν, cm^{-1}: 2940, 2870, 1720, 1692, 1650, 1605, 1580, 1400, 1340, 1315, 1275, 1230–1240, 1205, 1190, 1160, 1140, 1120, 1110, 1050, 1030, 985, 980, 950, 930, 910, 880, 850, 780, 750, 730, 710, 660, 640, 600, 590, 560, 505, 490, 460. ^{31}P–$\{^1H\}$ NMR spectrum (162.0 MHz, CCl_4): δ_P –16.3 ppm. Found, %: C 39.08; H 1.71. $C_{20}H_{10}\cdot F_{13}O_5P$. Calculated, %: C 39.47; H 1.64.

4,4-Bis(trifluoromethyl)-2-[1-methyl-1-(perfluorocyclohexyl)ethoxy]-6,7-benzo-1,3,2λ^5-dioxaphosphepin-5-one 2-oxide (XII). IR spectrum, ν, cm^{-1}: 1730, 1710 sh, 1660, 1620, 1590, 1570, 1520, 1385, 1307, 1290, 1250, 1220, 1185, 1160, 1125, 1080, 1045, 1015, 1000, 965, 930, 900, 860, 820, 789, 766, 730, 675, 656, 640, 620, 600, 565, 520, 489. ^1H NMR spectrum (300 MHz, acetone-d_6), δ, ppm (*J*, Hz): 1.98 br.d.m (CH_3, $^3J_{HCCH}$ 6.7) (d_2), 2.05 br.d.t (CH_3, $^3J_{HCCH}$ 6.6, $^4J_{POCCH}$ 1.9, $^4J_{FCCCH}$ 1.9) (d_1), 6.0–6.07 m (CH, $^3J_{HCCH}$ 6.6–6.7, $^4J_{FCCCH}$ 1.9) (d_1, d_2), 7.62 br.d.d.d (H^8, $^3J_{H^8CCH^9}$ 8.1, $^4J_{H^8CCCH^{10}}$ 1.5, $^4J_{POCCH}$ 1.3) (d_2), 7.71 d.d.d (H^8, $^3J_{H^8CCH^9}$ 8.2, $^4J_{H^8CCCH}$ d_1 1.4, $^4J_{POCCH}$ 1.2) (d_1), 7.78–7.79 m (H^{10},

$^{3}J_{H^{10}CCH^{11}}$ 7.8, $^{3}J_{H^{9}CCH^{10}}$ 7.4, $^{4}J_{H^{8}CCCH^{10}}$ 1.4, $^{6}J_{POCCCCH}$ 1.2) (d_1, d_2), 8.01 and 8.02 two d.d (H^{11}, $^{3}J_{H^{10}CCH^{11}}$ 7.8, $^{4}J_{H^{9}CCCH^{11}}$ 1.7) (d_1, d_2), 8.11–8.12 m (H^{9}, $^{3}J_{H^{8}CCH^{9}}$ 8.2, $^{4}J_{H^{9}CCCH^{11}}$ 1.7, $^{5}J_{POCCH}$ 1.2) (d_1, d_2). *Diastereomeric mixture.* $^{31}P-\{^{1}H\}$ NMR spectrum (162.0 MHz, $CDCl_3$), δ_P, ppm: –15.85 and –16.62. *Isolated diastereomer.* mp 48–50°C (from acetone). $^{31}P-\{^{1}H\}$ NMR spectrum: δ_P –16.31 ppm. Found, %: C 32.45; H 1.08. $C_{18}H_8F_{17}O_5P_4$. Calculated, %: C 32.83, H 1.22.

ACKNOWLEDGMENTS

The work was financially supported by the Program for Support of Leading Scientific Schools of Russia (project no. 00-15-97 424), Russian Foundation for Basic Research (project no. 02-03-32 280), and *Universities of Russia* Program (UR.05.01.016).

REFERENCES

1. Mironov, V.F., Burnaeva, L.A., Konovalova, I.V., Khlopushina, G.A., Mavleev, R.A., and Chernov, P.P., *Zh. Obshch. Khim.*, 1993, vol. 63, no. 1, pp. 25–32.
2. Mironov, V.F., Burnaeva, L.M., Konovalova, I.V., Khlopushina, G.A., and Chernov, P.P., *Zh. Org. Khim.*, 1993, vol. 29, no. 3, pp. 639–642.
3. Mironov, V.F., Mavleev, R.A., Burnaeva, L.A., Konovalova, I.V., Pudovik, A.N., and Chernov, P.P., *Izv. Ross. Akad. Nauk, Ser. Khim.*, 1993, no. 3, pp. 565–567.
4. Mironov, V.F., Burnaeva, L.M., Gubaidullin, A.T., Litvinov, I.A., Konovalova, I.V., Zyablikova, T.A., Ivkova, G.A., and Pomanov, S.V., *Zh. Obshch. Khim.*, 1998, vol. 68, no. 3, pp. 399–409.
5. Mironov, V.F., Gubaidullin, A.T., Litvinov, I.A., Burnaeva, L.M., Zyablikova, T.A., Khlopushina, G.A., and Konovalova, I.V., *Zh. Obshch. Khim.*, 1998, vol. 68, no. 4, pp. 567–602.
6. Mironov, V.F., Litvinov, I.A., Gubaidullin, A.T., Aminova, R.M., Burnaeva, L.M., Azancheev, N.M., Filatov, M.E., and Konovalova, I.V., *Zh. Obshch. Khim.*, 1998, vol. 68, no. 7, pp. 1080–1095.
7. Litvinov, I.A., Mironov, V.F., Gubaidullin, A.T., Konovalov, A.I., Ivkova, G.A., and Kurykin, M.A., *Zh. Obshch. Khim.*, 1999, vol. 69, no. 5, pp. 776–798.
8. Burnaeva, L.M., Gubaidullin, A.T., Mironov, V.F., Litvinov, I.A., Romanov, S.V., Konovalova, I.V., Zyablikova, T.A., and Pudovik, A.N., *Zh. Obshch. Khim.*, 2000, vol. 70, no. 8, pp. 1284–1293.
9. Burnaeva, L.M., Mironov, V.F., Romanov, S.V., Ivkova, G.A., Shulaeva, I.L., and Konovalova, I.V., *Zh. Obshch. Khim.*, 2001, vol. 71, no. 3, pp. 525–526.
10. Mironov, V.F., Litvinov, A.I., Gubaidullin, A.T., Konovalova, I.V., Zyablikova, T.A., Burnaeva, L.M., Romanov, S.V., and Azancheev, N.M., *Zh. Obshch. Khim.*, 2000, vol. 70, no. 11, pp. 1812–1832.
11. Mironov, V.F., Gubaidullin, A.T., Burnaeva, L.M., Litvinov, I.A., Brazhnikova, I.A., Mastryukova, T.A., Goryunov, E.I., and Konovalova, I.V., Abstracts of Papers, *Yubileinaya sessiya "Gorizonty organicheskoi I elementoorganicheskoi khimii"* (Anniversary Session "Horizons of Organic and Organoelement Chemistry"), Moscow, 1999, vol. II, R70, p. 72; Mironov, V.F., Burnaeva, L.M., Gubaidullin, A.T., Litvinov, I.A., Mastryukova, T.A., Goryunov, E.I., Konovalova, I.V., and Brazhnikova, I.A., Abstract of Papers, *XII Int. Conf. on the Chemistry of Phosphorus Compounds*, Kiev, 1999, p. 106; Burnaeva, L.M., Mironov, V.F., Konovalova, I.V., Goryunov, E.I., Mastryukova, T.A., Gubaidullin, A.T., Litvinov, I.A., and Yachagina, O.V., Abstracts of Papers, *XV Int. Conf. on Phosphorus Chemistry (ICPC16)*, Sendai (Japan), 2001, PB040, p. 220.
12. Mironov, V.F., Konovalova, I.V., Mavleev, R.A., Mukhtarov, A.Sh., Ofitserov, E.N., and Pudovik, A.N., *Zh. Obshch. Khim.*, 1991, vol. 61, no. 10, pp. 2150–2154; Mironov, V.F., Ofitserov, E.N., and Pudovik, A.N., *J. Fluorine Chem.*, 1991, vol. 54, nos. 1–3, p. 299; Mironov, V.F., Burnaeva, L.A., Konovalova, I.V., Khlopushina, G.A., and Zyablikova, T.A., *Zh. Obshch. Khim.*, 1995, vol. 65, no. 12, pp. 1986–1990; Mironov, V.F., Burnaeva, L.M., Gubaidullin, A.T., Brazhnikova, I.A., Litvinov, I.A., Romanov, S.V., and Konovalova, I.V., *Zh. Obshch. Khim.*, 2000, vol. 70, no. 10, pp. 1637–1644.
13. Mironov, V.F., Gubaidullin, A.T., Ivkova, G.A., Litvinov, I.A., Buzykin, B.I., Burnaeva, L.M., and Konovalova, I.V., *Zh. Obshch. Khim.*, 2001, vol. 71, no. 3, pp. 457–465.
14. Aminova, R.M., Mironov, V.F., and Filatov, M.E., *Zh. Obshch. Khim.*, 1999, vol. 69, no. 1, pp. 58–67.
15. Kirby, A., *The Anomeric Effect and Related Stereoelectronic Effects of Oxygen*, Heidelberg: Springer, 1983.
16. Cremer, D. and Pople, J.A., *J. Am. Chem. Soc.*, 1975, vol. 97, no. 6, pp. 1354–1358.
17. Prasanna, M.D. and Guru Row, T.N., *Cryst. Eng. Comm.*, 2000, vol. 25, pp. 134–141.
18. Spek, A.L., *Acta Crystalogr., Sect. A*, 1990, vol. 46, no. 1, pp. 34–40.
19. Sharma, C.V.K., Griffin, S.T., and Rogers, R.D., *Chem. Commun.*, 1998, p. 215.
20. Desiraji, G.R., *Angew. Chem., Int. Ed. Engl.*, 1996, vol. 34, pp. 2311–2327.
21. Mironov, V.F., Litvinov, I.A., Shtyrlina, A.A., Gu-

baidullin, A.T., Petrov, R.R., Konovalov, A.I., Dobrynin, A.B., Zyablikova, T.A., Musin, R.Z., and Morozov, V.I., *Zh. Obshch. Khim.*, 2002, vol. 72, no. 11, p. 1868.

22. Frenkel, S., *J. Polym. Sci., Polym. Symp.*, 1977, vol. 61, pp. 327–350

23. Kabachnik, M.I., Zakharov, L.I., Goryunov, E.I., and Svoren', V.A., *Dokl. Akad. Nauk SSSR*, 1979, vol. 245, no. 1, pp. 125–127.

24. Altomare, A., Cascarano, G., Giacovazzo, C., and Viterbo, D., *Acta Crystallogr., Sect. A*, 1991, vol. 47, no. 4, pp. 744–748.

25. Straver, L.H. and Schierbeek, A.J., *MOLEN, Structure Determination System*, vol 1. *Program Description*, Nonius B.V., 1994.